Physical & virtual assessment methods for simulating thermal propagation at cell and battery pack level.

Devyanshu Kumar, Miquel Planells, Enric Aramburu, Didac Casanellas, Charalampos Tsimis

Body Performance & Battery Lab
Applus+IDIADA
PO Box 20 L'Albornar
E-43710, Santa Oliva (Spain)
Charalampos.tsimis@idiada.com

Abstract: Battery cell thermal runaway and the resulting thermal propagation in battery packs pose a significant safety risk that needs to be addressed by OEMs. Moreover, since 2021 different thermal regulations, such as GB 38031 or UN ECE R100.03, require thermal runaway tests to be performed for vehicle type-approval. This paper outlines the experimental setup designed by Applus+IDIADA for conducting thermal runaway tests on individual battery cells. The experimental data gathered was used to validate the numerical methodology at the cell level. Subsequently, the paper outlines the methodology employed to simulate thermal propagation at the battery pack level.

1 Introduction & motivation

Li-ion cells operate properly in controlled temperature conditions, however, if due to external or internal heating cell temperature reaches a specific threshold, a thermal runaway (TR) process is triggered [1], which means highly exothermic chemical reactions occur internally and a large amount of energy and gasses are released rapidly. Moreover, besides overheating cases, other possible causes of Li-ion TR are internal shortcuts due to mechanical damage or manufacturing defects, which means that even avoiding impacts or external overheating, TR can happen spontaneously at any time in the vehicle lifetime. Thus, engineers must assume that thermal runaway may occur eventually, and concentrate on minimising the risk that it poses by studying it during the initial design stages of the battery pack.

It is well known that whenever TR happens, this can produce a cascade effect on neighbouring cells, the power released by the initiation cell can produce the overheating of the neighbour cells and then generate secondary TR, and so on. The goal of battery designers is twofold, first to provide sufficient cooling at the cell level to minimise the probabilities of a TR starting due to the formation of hot spots, and second to delay the heat transfer phenomena during a TR event by employing different mitigation strategies, such as proper thermal insulation or efficient extraction of TR gases.

Information regarding the chemical composition of battery cells can help engineers better estimate the energy and materials released during a TR event, by relying on the principles of theoretical chemical reaction kinetics. However, this information is not readily available as it typically forms part of the intellectual property of the cell manufacturer. An alternative path is conducting physical tests and measurements, in which the cell is deliberately induced into TR through various methods, and the thermodynamic behaviour of the cell is assessed with the help of sensors.

This paper will first describe a complete methodology for characterising cells in the test bench by a newly developed test rig at Applus+IDIADA. It will then detail the CFD methodology that was developed to replicate this test rig for fine tuning the battery cell model. Finally, it will present a CFD methodology for simulating battery packs with cell temperature dependent boundary conditions, to ultimately study the impact of different mitigation measures that can minimize thermal runaway and its propagation hazards.

2 Cell Characterization test rig.

A vertical cylindrical reactor with a lower air inlet and upper exhaust outlet was designed to test battery cell TR events in controlled conditions. The main goal of this test rig was to characterise cell TR by monitoring the temperature of the cell and measuring the gasses generated, along with their temperature.

2.1 Reactor design

The enclosure (reactor) to perform TR at cell level was selected to be a 40 L cylinder from a mechanically modified compressor.

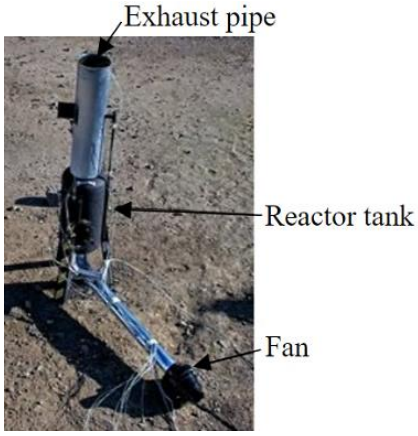

Figure 1: Reactor used for TR tests at cell level.

Both extremes of the cylinder were cut, and a ducting was attached before and after the reactor (Figure 1). At the bottom, a fan capable of circulating 200 m3/h was used to ensure continuous airflow; while at the top, an exhaust pipe of 20 cm diameter was

added, with a 10 mm diameter sampling point installed at 90 degrees. Several temperature sensors (Thermocouples Type K – fibre glass coated) were also added inside the reactor through a cable gland, as well as heating cables.

2.2 Cell selection

The cells used, as an example, in this paper to showcase the testing procedure and its subsequent replication in the CFD setup, were selected from a commercially available EV from 2022. The total energy of the battery pack was 52 kWh, with an individual cell energy of 440 Wh. Selected cells were prismatic and were recovered from a battery pack by dismantling the modules and accessing the individual cells. All plastic covers were removed, and cell walls were cleaned.

2.3 Cell assembly

Ceramic heaters were installed on the largest cell walls to trigger the cell thermal runaway. 4 heaters of 220 W were attached to the prismatic cell (2 on each face). Cell and heaters were assembled using metal grids (sandwich type configuration - Figure 2) and secured with springs. This let any potential cell expansion during TR to be allowed without putting stress on the cell. Thermocouples were added between the heater and the cells (T_{heater}) and on top of the larger cell wall, next to the heater (T_{case}).

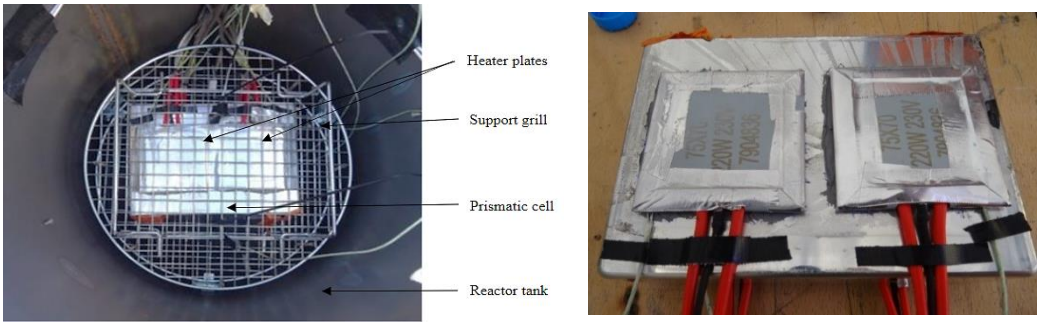

Figure 2: Cell assembly before TR tests, presented inside the reactor.

2.4 Data measurements

The gases released were estimated through the combination of three measurements. First the cell was weighted before and after the experiment to measure the total mass lost, second the exhaust gasses velocities were measured with the help of an anemometer positioned at the exit of the reactor tank, and third, the composition of the exhaust gasses was measured via the 10 mm diameter sampling point. Temperatures were monitored using thermocouples at key locations, including the

battery casing, heater plates, inlet and exit of reactor tank etc. In addition, a camera was installed to capture on video the detailed venting and runaway process. These measurements combined allowed to identify the TR onset temperature for cell-to-cell propagation and the venting phase.

On one hand the estimation of the gases released was used as an inlet boundary condition for the venting of hot gas in the simulations. On the other hand, the cell temperature measurements were used in an iterative, reverse engineering, process that helped determine the material properties (i.e. thermal conductivity & specific heat).

2.5 Test procedure

Constant heat flux was supplied to the battery cell through electric resistance, up to the point where smoke was detected. At that moment, the electric heaters were turned off and the ventilation fan was immediately activated to bring the cell back to ambient temperature.

3 CFD cell model

This section of the study focuses on finding key cell properties using an iterative CFD data-fitting approach. So, that further CFD thermal runaway analysis at battery module and/or pack level can be performed with greater accuracy. In the n*umerical model* of the physical experiment, a simplified, but full scale, model of the battery cell, heater-plates and reactor tank was considered (see figure 3). Thermocouples were placed at similar locations as they were in physical setup but the contact resistances between thermocouples, heater plates and cell casing were neglected (assumed zero thermal contact resistance). Also, the support grills and wiring connections were excluded in CFD modelling.

Commercial, STAR-CCM+ software was used as the CFD solver, with implicit unsteady modelling scheme. Turbulence was modelled with the K- ε, two-layer and All y+ model. Air was modelled as ideal gas and radiation was modelled with the surface-to-surface and gray thermal radiation models. Anisotropic thermal conductivity was assumed for the solid region representing the battery cell.

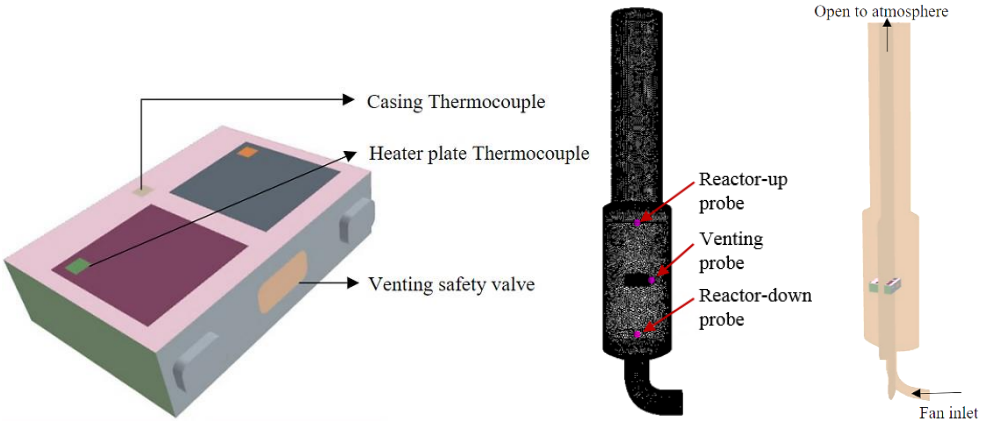

Figure 3: a) Cell geometry with heater plates and thermocouples; b) CFD simulation domain with surface mesh; c) Cut-section view highlighting the cell placement in the reactor tank.

3.1 Cell characterization methodology

In the current study, the actual prismatic cell was replaced by an equivalent lumped mass of same dimensions and attempts were made to find the equivalent thermal conductivity and specific-heat values for this rectangular mass.

In a usual CFD workflow the boundary conditions and material properties are provided, and with suitable modelling techniques, the desired flow field variables are obtained. In this study, initial simulation results were first obtained with some reference (/guessed) material properties of the battery cell. And then these characteristic properties were manually and iteratively adjusted to better match the experimental results.

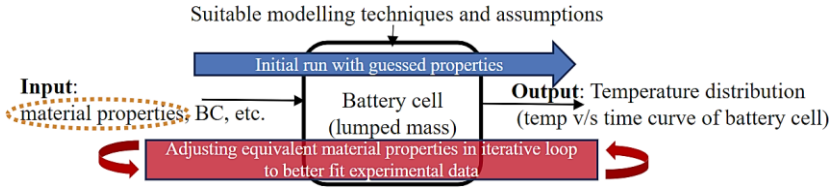

Figure 4: Illustration of CFD methodology for characterization of cell material properties.

The energy balance for this equivalent cell can be expressed as:

$$\rho_{eq}\, Cp_{eq} \left(\frac{\partial T}{\partial t}\right) = \nabla\left(K_{eq} \nabla T\right) + \phi$$

Where, ϕ is the additional source term accounting for the heat addition form heater plates and the internal heat generation during TR. The above equation also shows the relation between time rate of change of cell temperature and material properties,

which especially for low temperature ranges, becomes a strong function of thermal diffusivity, $\left(\frac{K_{eq}}{\rho Cp}\right)$; as radiation and natural convection currents are very small.

Due to the complexities in thermal runaway, the experimental data was analysed numerically in different phases, see figure 5.

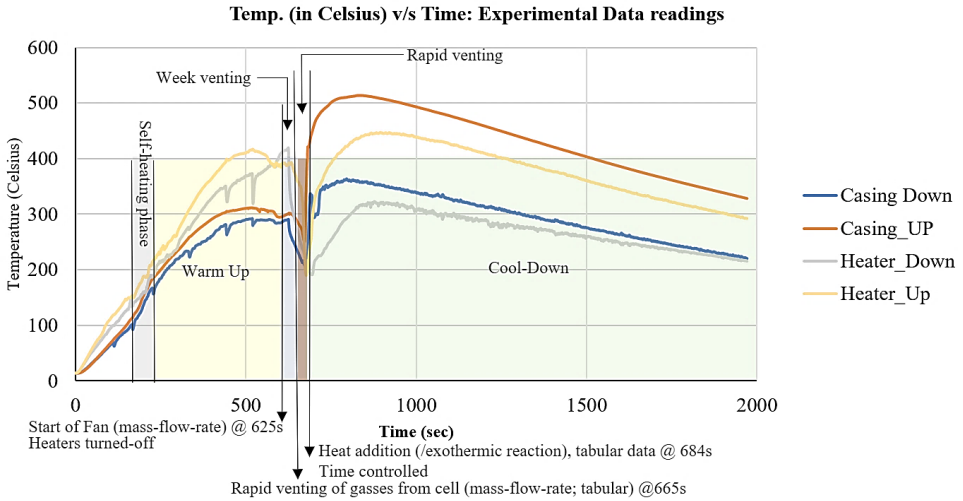

Figure 5: Breakdown of experimental data in multiple phases

3.1.1 Self-heating phase

A positive increase in the temperature gradient was observed (shown in fig. 5). Several literatures have identified the decomposition of SEI (Solid Electrolyte Interface) layer between temperature range of 90-120°C [2], resulting in exothermic reactions and hence the jump in the cell temperature. To depict this behaviour in simulation, a time-controlled total heat source was added to the cell region.

3.1.2 Warm-up phase

As the thermal abuse continued, cell underwent various physical and chemical changes. Polymer separator starts to melt (endothermic reaction) slowing down the rate of temperature increase. Moreover, as the temperature rises above 250°C decomposition of graphite anode with the electrolyte takes place [3], leading to exothermic chain reactions.

In this phase due to multiple reactions' (endo/exothermic) complexities, no additional heat generation was approximated, within the cell region. Cell temperature was allowed to increase solely due to the heater-plates.

3.1.3 Weak venting phase

Due to the continuous abnormal heating by the heater plates, separator layer vaporizes (endothermic), allowing the cathode and anode to make contact with each other, resulting in internal short circuit. This leads to highly exothermic Thermal runaway with the visible venting of smoke from the cell.

The instant smoke was detected, the heater plates were turned off and ventilating fan was started. This fan flow was modelled as velocity inlet in simulation, based on the experimental readings of air velocity entering the reactor tank. Similarly, to the warm-up phase, no additional heat generation was included due to multiple reactions' (endo/exothermic) complexities.

3.1.4 Rapid venting phase

Cell had undergone thermal runaway and about 460g of mass was lost as gas release. No actual combustion was detected. This venting of gas was modelled as an additional air mass-flow-inlet from venting safety valve surface of cell (shown in figure 3.) into the main air domain, at temperature equals to instantaneous cell average temperature. However, no actual reduction in lumped mass (representing the cell) was considered.

Additional time varying total heat source table was applied to the cell region for highly exothermic thermal runaway.

3.1.5 Cool down phase

Cell temperature started to decrease under the influence of forced convection, but still active internal reactions were slowing down the effect of cooling. For this reason, heat source was also introduced in this phase to better match the observed temperature trend.

However, it is very evident from the figure 6 that, simulations results (solid lines, in figure 6.) are offset by 40-50°C from experimental results (dotted lines). This could be because, in experimental analysis the contact between the cell casing, thermocouples and heater-plates was highly disturbed due to the high temperature and burning effects during thermal runaway process (see figure 7). Moreover, the thermal effects of TR were also observed to be non-homogenous in the actual cell experiment (figure 7, shows prominent burning effects on one side of the cell).

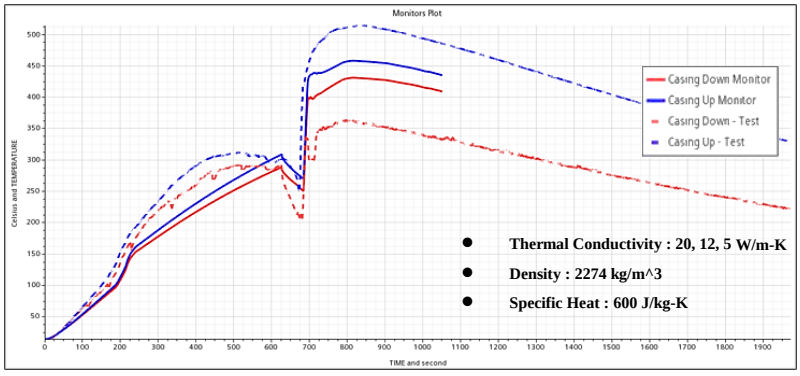

Figure 6: Experimental data of battery-casing temperature (up & down; dotted lines) v/s simulation results after iteratively correcting the material properties (solid lines)

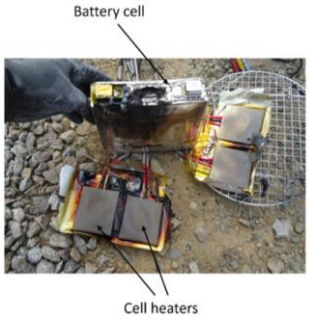

Figure 7: Battery cell and heaters after Thermal Runaway (TR) event.

As the current work shows, with suitable assumptions and proper analysis of experimental data this iterative approach has the potential to model virtually the battery cell as lumped mass and identify its equivalent material properties. The results from this method showed that an anisotropic thermal conductivity of 20, 12, 5 W/m-K (K_{xx}, K_{yy}, K_{zz}) and specific heat of 600 J/kg-K is better fitting the experimental data, for the cell tested, and the data fitting is within reasonable limits.

4 CFD battery model

Battery CFD models are used to study thermal propagation within the battery packs aiming to delay cell-to-cell propagation times by trying different materials, battery layouts, etc. In order to do so, the authors created a CFD model including a full module, composed by 6 prismatic cells and studied how adjacent cells are heated-up by convection, conduction and radiation, to identify the main energy exchange drivers. The battery pack example shown below (Figure 8) as proof of concept of the CFD methodology for thermal runaway simulation belongs to the Marbel EU project (https://marbel-project.eu/).

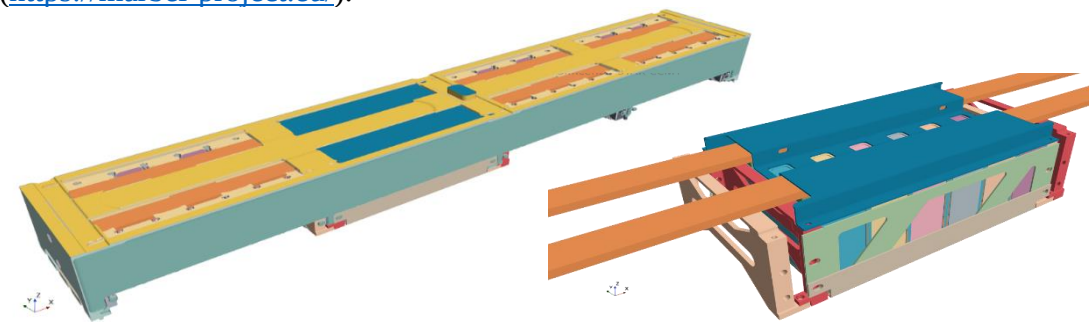

Figure 8: a) Battery pack (1 row), b) module (6 cells)

4.1 Case set-up

The cell characterization procedure described in chapters 2 and 3 is used to define the main cell parameters, regarding thermal conductivity, specific heat, energy and gas release. Energy and gas release are temperature- and time-dependent boundary conditions. The release of energy and gas happens when battery cells reach an onset temperature, which was identified in the cell characterization tests, and then follows a time-dependent curve. To mimic this behaviour in the CFD model, the authors used customized field functions to activate time-dependent tables (boundary conditions) instantaneously, as the monitor reaches threshold values. The maximum cell temperature is monitored cell-by-cell, individually, then when this temperature exceeds the onset temperature (150ºC), an inlet boundary condition, located on the cell burst membrane, is activated to inject hot venting gases (air) into the flow domain, along with a cell internal heat source with time-dependent definition.

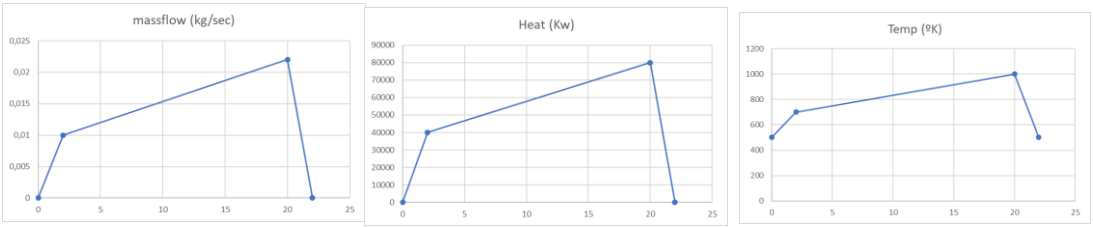

Figure 9: Cell time-dependent boundary conditions

Since the battery cell assumed in the Marbel battery pack was not available for testing using the procedure described in the first part of this paper, the internal heat generation and gas release quantities were initially set, based on the authors experience in testing similar chemistry batteries. Authors then amplified these theoretical values, reaching peak values to 80 kW of internal heat, 0,022 kg/s of gas release and 1.000º K for the gas temperature, in order to force thermal propagation within batteries and hence, to validate the methodology for simulating this propagation cascade effect. The time-dependent boundary conditions curves are presented in Figure 9.

The main material parameters of the module assembly were provided by the Marbel consortium and are shown in the figure 10, below.

As explained above, the first challenge was creating a temperature- and time-dependent cell set-up that leverages measurements obtained in the cell test rig. The second challenge was simulating a full battery test including a realistic battery pack capable to simulate up to 5’ of real time, with affordable computational resources. These challenges as well as the confidence level on the simulation depends very much on the spatial and temporal discretization, so the authors performed a sensitivity analysis regarding time-step and mesh refinement to ensure that CFD results do not depend on these model parameters.

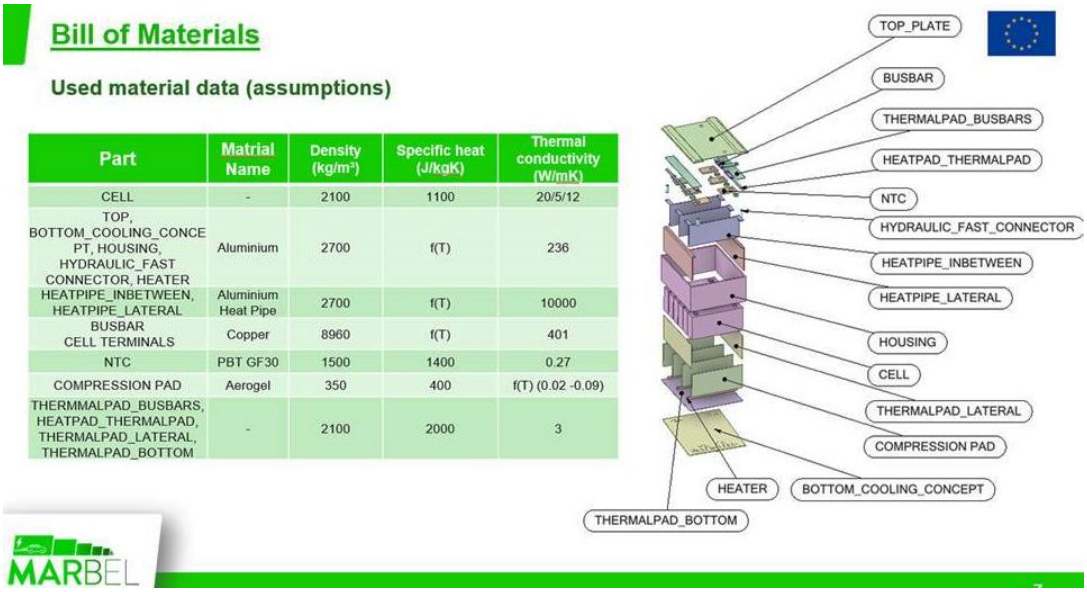

Figure 10: Material properties

4.2 CFD results

The authors monitored cell maximum temperatures in all the battery cells to compute cell-to-cell propagation time, which is deemed the main test KPI. The plots of these monitors are shown in the picture below (Figure 11). Looking at these results and checking when the onset temperature is reached, we can conclude that cell to cell propagation time of the example case is realized on average within 15 seconds. If the main venting period of this cell lasts 20" (fast venting), the authors understand that delaying the cell-to-cell propagation time to more than 20", for example 30", could help to contain TR to a single cell and interrupt thermal propagation to the entire battery.

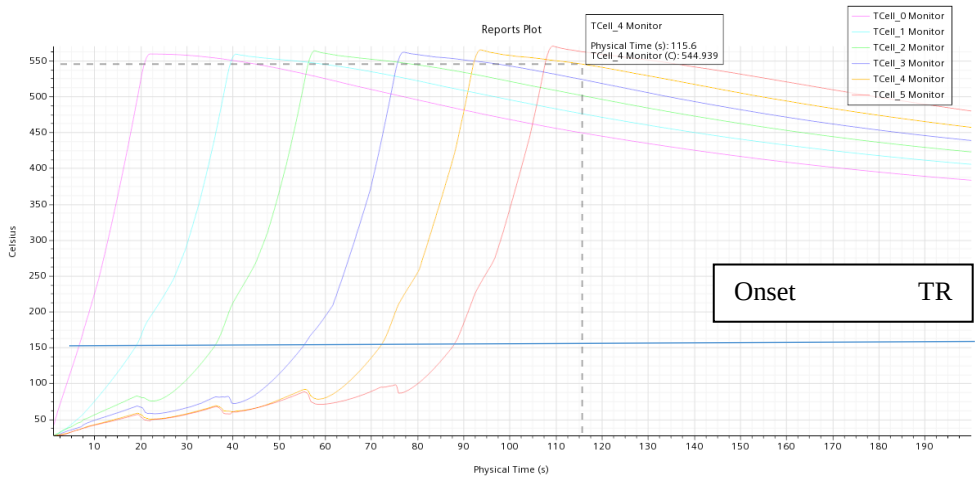

Figure 11: Maximum cell temperature plots

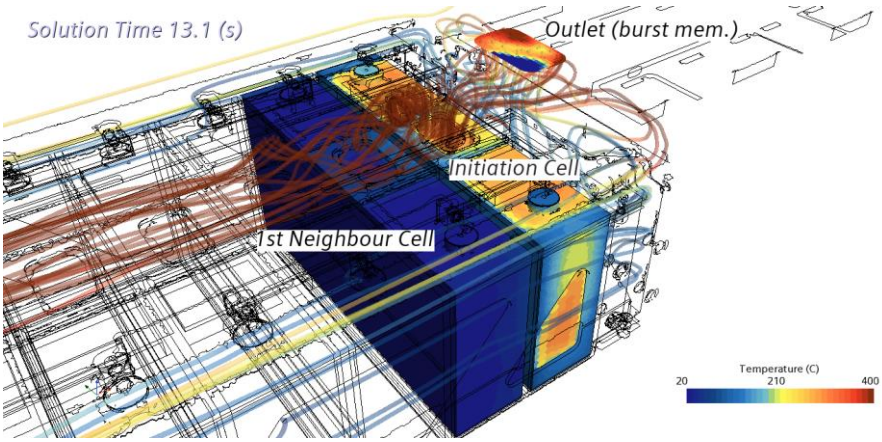

Figure 12: CFD results: cell temperature & streamlines

CFD analysis can be very useful to understand how batteries heat-up in TR tests. The energy exchange balance at the first cell next to the initiating cell can show how this cell heats-up and which are the main heat transfer paths (these results are presented in Table 1). Looking at this table, we can conclude that the main energy path is through the frame metal parts. Therefore, acting on that heat transfer path, we could delay the cell-to-cell propagation, for instance by adding a thermal insulation between the metal and the cell.

Table 1: Cell heat transfer paths

Heat transfer breakdown (Time = 13.1)	%
Flow domain	4%
Thermal pads	34%
Metal frames	62%
TOTAL	100%

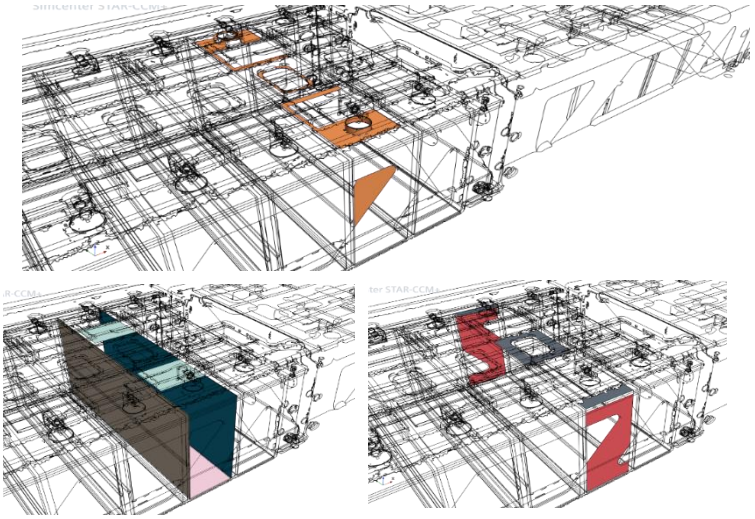

Figure 13: a) Flow domain patch, b) thermal pads patch, c) metal frames patches (grey & red)

5 Conclusions and future scope

The authors developed a complete methodology for simulating thermal propagation tests by means of CFD, which are helpful in the decision-making process at batteries design phases, furthermore the authors have proven its applicability at industrial level on a real test-case. This process includes a cell characterization test rig, a reverse engineering process for setting the cell parameters from test measurements, a CFD methodology for full battery pack thermal simulation and an analysis procedure to diagnose the neighbouring cell heating process during thermal propagation.

This CFD methodology is currently limited to fluid-dynamics and thermal analysis, further methodology developments could be introduced in the future for being more realistic, through adding more complexity in the CFD set-up, for instance: modelling of melting parts, deformation of structural parts, or secondary fire events and smoke modelling.

6 Bibliography

[1] V. Ruiz and A. Pfang, “JRC exploratory research: Safer Li-ion batteries by preventing thermal propagation,” European commision, 2018.

[2] H. Liu, Z. Wei, W. He and J. Zhao, Thermal issues about Li-ion batteries and recent progress in battery thermal; A review, Energy Conversion and Management, Elsevier, 2017.

[3] X. Feng, M. Ouyang, X. Liu, L. Lu, Y. Xia and X. He, Thermal runaway mechanism of lithium ion battery for electric vehicles: A reiew, Energy storage materials, Elsevier, 2017.